

and vibron frequencies at the pressure ranging from 0 to 3.0 GPa with the software package of the general utility lattice program (GULP).³⁻⁴⁾ The total potential V_{total} is described as the sum of intra- and intermolecular potentials,

$$V_{total} = \sum_{i=1}^N (V_{intra} + \frac{1}{2} \sum_{j=1}^N V_{inter}(r_{ij})) \quad (4)$$

The intermolecular potential consists of the superposition of a pairwise sum of Buckingham (6-exp) (repulsion and dispersion) and coulombic potentials (V^c) of the form:

$$V_{\alpha\beta}(r_{\alpha\beta}) = A_{\alpha\beta} \exp(-B_{\alpha\beta} r_{\alpha\beta}) - \frac{C_{\alpha\beta}}{r_{\alpha\beta}^6} \quad (5)$$

and,

$$V_{\alpha\beta}^c(r_{\alpha\beta}) = \frac{q_{\alpha} q_{\beta}}{4\pi\epsilon_0 r_{\alpha\beta}} \quad (6)$$

where $r_{\alpha\beta}$ is the interatomic distance between the atoms α and β belonging to different molecules, q_{α} and q_{β} are the corresponding electrostatic charges on these atoms, and ϵ_0 is the dielectric permittivity constant for free space. The parameters $A_{\alpha\beta}$, $B_{\alpha\beta}$ and $C_{\alpha\beta}$ for different types of atomic pairs have been previously published⁵⁾ and have been used in the present study without change except for the N...H atomic pairs. The atomic pair of N...H intermolecular potential were refitted to reproduce the experimental structure. The values of the intermolecular potential parameters are given in Table 1.

The set of partial charges used in these calculations were determined through fitting these to the quantum-mechanically-derived electrostatic interaction potential for an isolated molecule whose atoms are rearranged

according to the experimental crystallographic structure. These calculations have been done using the CHELPG procedure as implemented in the Gaussian 98 package⁶⁾ in conjunction with Møller-Plesset perturbation theory at the MP2/6-31G** level.

The intramolecular potentials were assumed the form as follows:

$$V_{intra} = \sum V_{bond} + \sum V_{angle} + \sum V_{torsion} + \sum V_{nonbond} \quad (7)$$

to describe the bond stretching, angle bending, torsional motions and nonbonded interactions that occur within an isolated molecule. The covalent bond stretch can be approximated as a harmonic oscillator,

$$V_{bond} = \frac{1}{2} k_r (r - r_0)^2 \quad (8)$$

where r is the bond distances, r_0 is the equilibrium bond length and k_r is the force constant describing the stiffness of the bond.

The angle-bending potential is represented by the form.

$$V_{angle} = \frac{1}{2} k_{\theta} (\theta - \theta_0)^2 \quad (9)$$

where k_{θ} is the force constant and θ_0 is the equilibrium value of the angle.

The torsional potential is represented by the form

$$V_{torsion} = V_{\phi} (1 + i \cos(m(\Phi - \Phi_0))) \quad (10)$$

where V_{ϕ} is a half of the intramolecular torsional barrier, Φ is the torsional angle, and $m = 1, 2, 3$, or 4, and i is +1 or -1 according to the sign of m phase.

Nonbonded interactions are considered intramolecularly for all atoms separated by three or more bonds in

Table 1 The intermolecular atom-atom potential parameters for PETN^a

Pair ($\alpha - \beta$)	$A_{\alpha\beta}$ (KJ/mol)	$B_{\alpha\beta}$ (\AA^{-1})	$C_{\alpha\beta}$ (KJ/mol)
H - H	9213.510	3.74	136.3800
C - C	369726.330	3.60	2439.3459
N - N	264795.246	3.78	1668.3316
O - O	290437.820	3.96	1453.3114

^a With the exception of pair of N - H, for pairs of unlike atoms, $A_{\alpha\beta}$, $B_{\alpha\beta}$ and $C_{\alpha\beta}$ were calculated from the formulae $A_{\alpha\beta} = (A_{\alpha\alpha} A_{\beta\beta})^{1/2}$, $B_{\alpha\beta} = (B_{\alpha\alpha} + B_{\beta\beta})/2$, $C_{\alpha\beta} = (C_{\alpha\alpha} C_{\beta\beta})^{1/2}$.
 $A_{N-H} = 444979.009$ KJ/mol, $B_{N-H} = 3.76 \text{ \AA}^{-1}$, $C_{N-H} = 2310.1980$ KJ/mol.

Table 2 The force constants of the intramolecular potential Parameters for PETN.^a

Bond Stretching Parameters			angle bending parameters		
Bond	k_r (KJ mol ⁻¹ Å ⁻²)	r_0 (Å)	Angle	k_θ (KJ mol ⁻¹ rad ⁻²)	θ (deg)
N-O	3765.66	1.217	C-C-C	334.72	109.5
N-O _s	2510.44	1.389	C-C-H	418.41	110.4
C-C	2594.13	1.538	C-C-O _s	418.41	107.6
C-H	2941.65	1.03	H-C-O _s	418.41	108.7
C-O _s	2677.81	1.433	H-C-H	292.89	111.4
			O-N-O _s	585.77	115.98
			O-N-O	585.77	127.80
			C-O _s -N	585.77	117.7

Torsion potential parameters				
Dihedral angle	V_ϕ (KJ/mol)	δ (deg)	M	i
O-N-O _s -C	3.7658	0.0	2	-1
C-C-C-O _s	37.658	0.0	3	+1
N-O _s -C-C	-4.8117	0.0	3	-1
H-C-C-C	0.4824	0.0	2	+1

Nonbonded potential $V_{\alpha\beta}^{LJ}(r) = \epsilon_{\alpha\beta} [(r_0/r_{\alpha\beta})^{12} - 2(r_0/r_{\alpha\beta})^6]$					
Pair ($\alpha - \beta$)	ϵ (KJ)	r_0 (Å)	Pair ($\alpha - \beta$)	ϵ (KJ)	r_0 (Å)
C ₁ -C ₁	0.25104	3.60	C ₂ -C ₂	0.37656	3.70
H-H	0.04184	3.08	O _s -O _s	0.62760	3.30
O-O	0.8368	3.20	N-N	0.66944	3.50

^a for pairs of unlike atoms, $r_{\alpha\beta}^0$ and $\epsilon_{\alpha\beta}$ were calculated from the formulae $r_{\alpha\beta}^0 = (r_{\alpha\alpha}^0 + r_{\beta\beta}^0)/2$, $\epsilon_{\alpha\beta} = (\epsilon_{\alpha\alpha} \epsilon_{\beta\beta})^{1/2} (r_{\alpha\alpha}^0 r_{\beta\beta}^0)^3 / (r_{\alpha\beta}^0)^6$.

PETN molecules. The potential is represented by the Lennard-Jones form.

$$V_{\alpha\beta}^{LJ}(r_{\alpha\beta}) = \epsilon_{\alpha\beta} \left[\left(\frac{r_{\alpha\beta}^0}{r_{\alpha\beta}} \right)^{12} - 2 \left(\frac{r_{\alpha\beta}^0}{r_{\alpha\beta}} \right)^6 \right] \quad (11)$$

All force-field parameters in expressions (8) – (11) are taken directly from the earlier literature.⁷ The values of these parameters are given in Table 2.

3. Results and discussion

At normal pressures, PETN is known to exist in two phases in the temperature range from zero to the melting point (416K): a tetragonal phase also called form I⁸) and an orthorhombic phase known as form II⁹). PETN I is thought to be the most stable form. PETN II can exist at temperature above 403 K and transform rapidly to PETN I below 403 K. As determined by x-ray diffraction measurements, the space group for PETN I is $P\bar{4}2_1c$ with two molecules per unit cell, while $Pcnc$ with four molecules per unit cell for PETN II.

The lattice constants are evaluated by minimizing the

total crystal potential energy, while varying the lattice parameters, a , b , and c , as well as the orientations of the atoms in the unit cell. The unit cell angles remain 90° to be consistent with the space group symmetry. The minimized configurations have been verified by phonon calculations that the first three vibrational frequencies are equal to zero and all of other frequencies have positive values, indicating the existence of a local minimum.

3. 1 Lattice properties

The accuracy of the flexible potentials was checked by comparing the calculated lattice properties with experimental values. Resulting lattice parameters and lattice energy are listed in Table 3. The maximum deviation in the lattice dimensions is 4.1%. At ambient pressure, not only total lattice energy, but also elastic constants are in excellent agreement with the available experiment data¹⁰⁻¹¹). Recently, the entire set of elastic constants for single crystal PETN I have been measured by Gupta.¹¹ Comparison between experimental and calculated results is given in Table 4. It indicated that elastic constants can be predicted accurately by the

Table 3 Comparison of Calculated and Experimental lattice Parameters and Total Energy.

		$a(\text{\AA})$	$b(\text{\AA})$	$c(\text{\AA})$	$V(\text{\AA}^3)$	Lattice energy (kJ/mol)
PETN I	Exp.	9.38	9.38	6.71	590.375	-156.9 ^{a)}
	Calc	9.447	9.447	6.983	623.158	-157.08
PETN II	Exp.	13.29	13.49	6.83	1224.4967	—
	Calc	13.237	13.588	6.902	1241.4611	-157.66

^{a)} reference 10, the lattice energy is calculated using the relationship: $E = -\Delta H_{\text{subl}} - 2RT$, ΔH_{subl} is the experimental sublimation enthalpy, $T=298\text{K}$.

Table 4 The elastic constants for the optimized structure of PETN I (GPa)

	C_{11}	C_{22}	C_{33}	C_{44}	C_{55}	C_{66}	C_{12}	C_{13}	C_{23}
Exp	17.241	17.241	12.174	5.043	5.043	3.944	5.449	7.943	8.001
Calc	17.628	17.628	16.620	3.789	3.789	3.778	7.891	9.334	9.334

flexible potential used in the present work. Because the elastic constant matrix is symmetric, only the upper half is given in the table.

At high pressures, the crystal is slightly less compressible for the present potential than the shock compression experiments.¹²⁻¹³⁾ At the pressure of 3.0 GPa, the present volume compressibility (V/V_0) is 0.88, which is comparable to 0.86 obtained by the shock compression experiments.¹²⁻¹³⁾

We used Murnaghan equation to fit the dependence of the unit cell volume on pressure.

$$P(V) = \frac{B_0}{B_0'} \left[\left(\frac{V_0}{V} \right)^{B_0'} - 1 \right] \quad (12)$$

where B_0 is the bulk modulus at zero pressure, B_0' is the pressure derivative of B_0 , $B_0' = \left. \frac{dB_0}{dP} \right|_{P=0}$. The fitted

parameters are $B_0 = 12.99$ GPa, $B_0' = 8.51$ for PETN I, comparable with the experimental value of $B_0 = 9.85$ GPa and $B_0' = 8.75$ based on Hugoniot data¹³⁾. For PETN II, $B_0 = 14.02$ GPa and $B_0' = 8.07$.

Experimentally, Bulk modulus B_0 and the pressure derivative B_0' in eq.(12) can be calculated in terms of Hugoniot-Rankine relations, where U_s is the shock velocity and U_p is the particle velocity.

$$P = \rho_0 U_s U_p \quad (13)$$

$$\frac{V}{V_0} = 1 - \frac{U_p}{U_s} \quad (14)$$

For single crystal PETN I, the shock-particle velocity Hugoniot may be given by¹³⁾,

$$U_s = 2.320 + 2.61U_p - 0.38U_p^2, \quad U_s \leq 4.1648 \text{ km/s}$$

$$U_s = 2.811 + 1.73U_p, \quad U_s \geq 4.195 \text{ km/s}$$

Corresponding B_0 and B_0' are 9.85 GPa, 8.75 for $U_s \leq 4.1648 \text{ km/s}$ ($P \leq 5.91$ GPa) and 13.99 GPa, 5.94 for $U_s \geq 4.195 \text{ km/s}$ ($P \geq 5.95$ GPa).

3. 2 Pressure dependence of phonon and vibron frequency

There are few studies about vibrational spectrum of PETN due to its complex structure. Recently, Gupta et al¹⁴⁾ have calculated the vibrational frequency and assigned normal mode vibrations using density functional theory (DFT) calculations at the B3LYP/6-31G(d) and B3LYP/6-311+G(d,p) level. Based on a group theory, the numbers of vibrons and phonons (including Davydov splittings) are 81×2 and 9 for PETN I crystal and 81×4 and 21 for PETN II crystal, where 81 represents the number of internal vibrational modes for isolated molecule. We have calculated the frequency for these phonons and vibrons at the pressure ranging from 0 - 3.0 GPa. Compression of a crystal induces frequency shifts in the both phonon and vibrational modes. Generally, the shifts for phonon modes are much greater than the shifts for vibrational modes. An example of

frequency changing with volume is shown in Fig. 1.

The molecular point group for isolated PETN I molecule is S_4 with irreducible representations of $\Gamma_g = 20A+21B+20E$. The 20A modes are not IR active and the

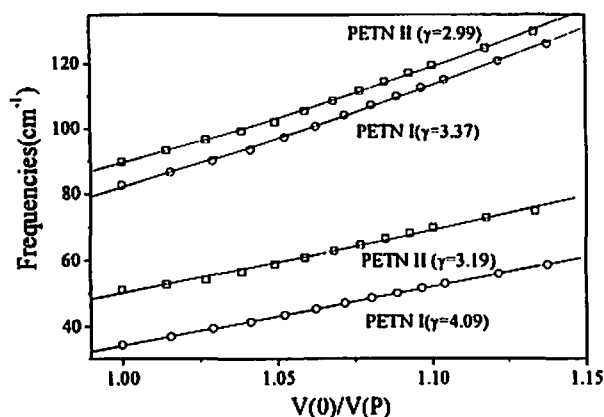


Fig.1 The frequencies shift of phonons plotted against volume change.

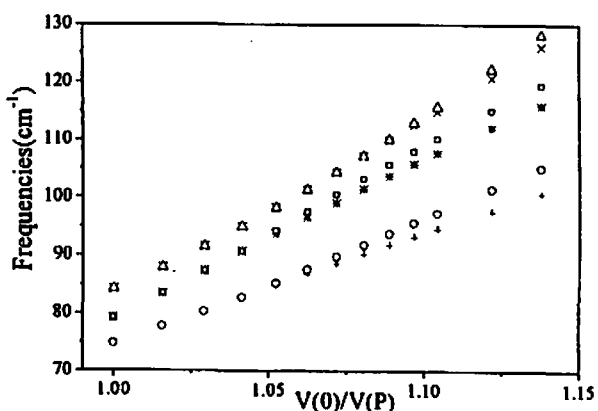


Fig.2 The splitting of the generate modes of PETN I.

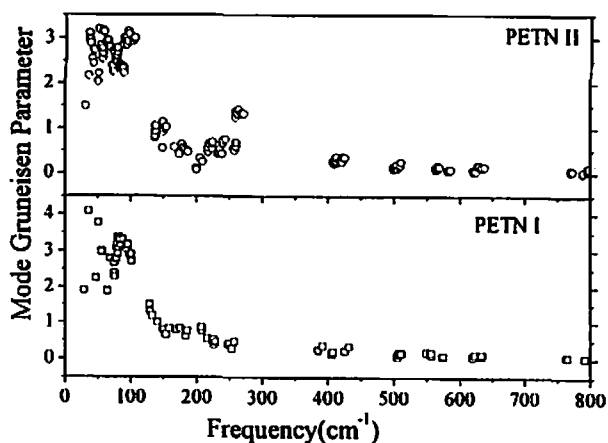


Fig.3 The calculated mode Grüneisen coefficients γ_i for the modes below 800cm^{-1} .

20E modes are doubly degenerated. For these degenerate modes, splitting is occurred to some modes with pressure increasing, as shown in Fig. 2.

3. 3 Mode Grüneisen coefficients γ_i

We calculated γ_i using Eq.(3). The results for the modes below 800cm^{-1} are shown in Fig. 3. For PETN I, γ_i of values are ranging from 1.88 to 4.09 for the modes at the frequencies below 110cm^{-1} , while the values are less than 1.55 above 110cm^{-1} . For PETN II, γ_i are ranging from 1.5 to 3.19 for the modes at the frequencies below 110cm^{-1} and are less than 1.45 above 110cm^{-1} . However, γ_i of the modes with frequencies larger than 550cm^{-1} are less than 0.2 for PETN I and PETN II. The modes with largest Grüneisen coefficient are located at 35.1cm^{-1} for PETN I ($\gamma_i = 4.09$) and 50.8cm^{-1} for PETN II ($\gamma_i = 3.19$). With the passage of the shock front, the mode at 35.1cm^{-1} in PETN I crystal and 50.8cm^{-1} in PETN II are excited more easily than other modes.

In PETN crystal, there are many low frequency vibrational modes involving NO_2 rocking motions and ONO_2 wagging motions. Gupta et al. observed that there are 10 vibrational modes below 100cm^{-1} (not include Davydov splitting).¹⁴⁾ These low frequency vibrational modes amalgamate with phonon modes and have a considerable large value of γ_i , equal to or slightly smaller than γ_i for pure phonon modes, but much larger than γ_i for high-frequency vibrational modes. The considerable large value of γ_i indicate that the amalgamated modes can be easily excited by the shock. Thus we assign the amalgamated vibrations as phonon modes. The averaged value of γ_i for the modes below 110cm^{-1} are 2.94 and 2.69 for PETN I and PETN II, respectively.

In addition, Nagayama et al.¹⁵⁻¹⁶⁾ have developed a new method for calculating the bulk Grüneisen parameter using Hugoniot data. Subsequently they studied Grüneisen paramter and thermal nonequilibrium of polymers. The $U_s - U_p$ Hugoniot curve of the polymers they considered exist a sharp kink.¹⁷⁾ Their results suggested larger Grüneisen parameter at low-pressure side of the kink correspond to the values of microscopic Grüneisen coefficients for intermolecular phonon excitation and the shock waves are not in dynamical and thermal equilibrium. At high-pressure side of the kink shock waves approach thermal equilibrium, although are still not in dynamical equilibrium, which result in the decrease of Grüneisen parameter.

Table 5 Grüneisen parameter calculated by eq. (16)

	B_0 (GPa)	B_0	Γ_{Slater}	Γ_{DM}	Γ_{VZ}	$\bar{\gamma}_i (\omega \leq 110cm^{-1})$
PETN I (calc)	12.99	8.51	4.09	3.75	3.42	2.94
PETN I ($U_s \leq 4.1648km/s$)	9.85	8.75	4.21	3.87	3.54	—
PETN I ($U_s \geq 4.195km/s$)	13.99	5.94	2.80	2.47	2.14	—
PETN II (calc)	14.02	8.07	3.87	3.54	3.20	2.69

The method developed by Nagayama is based on the theoretical models proposed by Slater¹⁸⁾, Dugdale and MacDonald (DM)¹⁹⁾, Vaschenko and Zubarev (VZ)²⁰⁾. The three models may be conveniently represented by the following single equation,

$$\Gamma = -\frac{V}{2} \frac{\frac{d^2}{dV^2}(PV^{2t/3})}{\frac{d}{dV}(PV^{2t/3})} + \frac{t-2}{3} \quad (15)$$

where parameter t is 0, 1, 2 for the Slater, DM and VZ models, respectively.

Based on Murnaghan equation, eq.(15) may be rewritten as,

$$\Gamma = -\frac{1}{2} \frac{\left(\frac{V_0}{V}\right)^{2t} \left(\frac{2t}{3} - B_0\right) \left(\frac{2t}{3} - B_0 - 1\right) - \frac{2t}{3} \left(\frac{2t}{3} - 1\right)}{\left(\frac{V_0}{V}\right)^{2t} \left(\frac{2t}{3} - B_0\right) - \frac{2t}{3}} + \frac{t-2}{3} \quad (16)$$

Grüneisen parameters calculated using eq.(16) are given in Table 5. The averaged value of the modes in phonon region ($\bar{\gamma}_i (\omega \leq 110cm^{-1})$) is listed out for comparison. The value of Γ calculated using eq.(16) is larger than $\bar{\gamma}_i (\omega \leq 110cm^{-1})$. As pointed out by Nagayama, et al¹⁵⁾, although none of the three models are applied to any solid materials, Grüneisen coefficients is still estimated roughly by these models. The value of Γ for PETN I is similar to the value based on shock Hugoniot data for $U_s \leq 4.1648 km/s$, which corresponds $P \leq 5.9 GPa$, but much larger than the value for $U_s \geq 4.195 km/s$ ($P \geq 5.9 GPa$). The value of Γ for PETN II is less than Γ for $U_s \leq 4.1648 km/s$ and larger than Γ for $U_s \geq 4.195 km/s$.

3. 4 Shock-induced temperature increase

To simplify the calculations of the shock temperature,

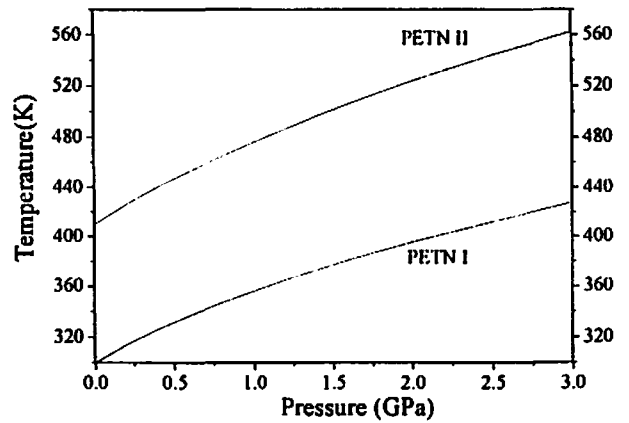


Fig.4 Calculated shock temperature as a function of pressure.

we ignore the irreversible part of eq. (1). Shock temperature increase (relative to an initial temperature taken to be $T_0 = 300 K$ for PETN I and $T_0 = 410 K$ for PETN II) is plotted in Fig. 4 for hydrostatic bulk volume compression as a function of pressure, assuming that the bulk Grüneisen parameter is constant at different pressure and approximate to the averaged value of the modes in phonon region ($\bar{\gamma}_i (\omega \leq 110cm^{-1})$ in Table 5). For shock pressure of 3.0 GPa, temperature of PETN I and PETN II jump to 427 K and 563 K, respectively. Since the compressibility depends strongly on crystal orientation, the shock temperature for the compression of bulk volume is different for the compression along a, b and c axes.

Dick et al have observed that the shock initiation of PETN is very sensitive to crystal orientation.²¹⁾ The most sensitive orientation for PETN I is [110] plane. This effect was explained in terms of a geometric analysis of the steric hindrance to shear in the uniaxial strain of a shock wave. Gupta et al measured the temperature increase at this stress for 5.0 GPa based on the antistokes and stokes scattering intensities. The temperature increase at [110] and [001] plane is estimated on the order of 100 K for $P=5.0 GPa$.²²⁾ For this temperature increase, the

shock front of PETN I is possible to transform into PETN II before thermal equilibrium is reached. Maienschein et al studied the effect of microvoids on the shock initiation of PETN and observed an unexpected pressure release in pure PETN shocked to 2 GPa. They tentatively interpreted as a shock-induced phase change.²³⁾ But very few experimental evidences support the phase change of PETN I.

4. Conclusion

We have used a flexible potential containing both intra- and intermolecular potential to calculate the pressure dependence of phonon and vibron frequency shifts of two polymorphs of Pentaerythritol Tetranitrate (PETN) at the pressure ranging from 0 to 3.0 GPa. The flexible potentials can predict the lattice properties accurately. Resulting mode Grüneisen coefficients are in the range from 1.88 to 4.09 for the modes in phonon region ($\omega \leq 110 \text{ cm}^{-1}$) of PETN I, and from 1.5 to 3.19 for PETN II. The averaged Grüneisen coefficients of the modes in phonon region is 2.94 and 2.69 for PETN I and PETN II, respectively. In PETN I and PETN II, mode Grüneisen coefficients are less than 1.55 for the modes with the frequency of 110 – 550 cm^{-1} , and less than 0.2 for the modes below 550 cm^{-1} .

A shock temperature was calculated using the averaged Grüneisen coefficients of the modes in phonon region. The temperature increase is estimated on the order of 100 K at $P = 3.0$ GPa for the bulk volume compression.

References

- 1) A. Tokmakoff, M. D. Fayer, D. D. Dlott, *J. Phys. Chem.* 97:1901 (1993).
- 2) V. K. Jindal, D. D. Dlott, *J. Appl. Phys.* 83: 5203 (1998).
- 3) J. D. Gale, *Philos. Mag. B*, 73: 3 (1996).
- 4) J. D. Gale, *J. Chem. Soc., Faraday Trans.* 93: 629 (1997).
- 5) D. C. Sorescu, B. M. Rice, D. L. Thompson, *J. Phys. Chem. B*, 101: 798 (1997).
- 6) Gaussian 98 (Revision A.7), M. J. Frisch, G. W. Trucks, H. B. Schlegel, G. E. Scuseria, M. A. Robb, J. R. Cheeseman, V. G. Zakrzewski, J. A. Montgomery, Jr., R. E. Stratmann, J. C. Burant, S. Dapprich, J. M. Millam, A. D. Daniels, K. N. Kudin, M. C. Strain, O. Farkas, J. Tomasi, V. Barone, M. Cossi, R. Cammi, B. Mennucci, C. Pomelli, C. Adamo, S. Clifford, J. Ochterski, G. A. Petersson, P. Y. Ayala, Q. Cui, K. Morokuma, D. K. Malick, A. D. Rabuck, K. Raghavachari, J. B. Foresman, J. Cioslowski, J. V. Ortiz, A. G. Baboul, B. B. Stefanov, G. Liu, A. Liashenko, P. Piskorz, I. Komaromi, R. Gomperts, R. L. Martin, D. J. Fox, T. Keith, M. A. Al-Laham, C. Y. Peng, A. Nanayakkara, C. Gonzalez, M. Challacombe, P. M. W. Gill, B. Johnson, W. Chen, M. W. Wong, J. L. Andres, C. Gonzalez, M. Head-Gordon, E. S. Replogle, and J. A. Pople, Gaussian, Inc., Pittsburgh PA, 1998.
- 7) S. J. Weiner, P. A. Kollman, D. T. Nguyen, D. A. Case, *J. Comp. Chem.*, 7: 230 (1986).
- 8) J. Trotter, *Acta Cryst.*, 16: 698 (1963).
- 9) H. H. Cady, A. C. Larson, *Acta Cryst. B*, 31: 1864 (1975).
- 10) J. S. Chickos, In *molecular Structure and Energetics*; J. F. Liebman, A. Greenberg, Eds.; VCH Publishers Inc.: New York, 1987; Vol. 2.
- 11) J. M. Winey, and Y. M. Gupta, *J. Appl. Phys.* 90: 1669 (2001).
- 12) B. Olinger, P. M. Halleck, and H. H. Cady, *J. Chem. Phys.* 62: 4480 (1975).
- 13) B. M. Dobratz, P. C. Crawford, "LLNL Explosives Handbook, Properties of Chemical Explosives and Explosive Simulants", UCRL-52997, Change 2, 1985, Lawrence Livermore National Laboratory.
- 14) Y. A. Gruzdikov, Y. M. Gupta, *J. Phys. Chem. A*, 105: 6197 (2001).
- 15) K. Nagayama, Y. Mori, *J. Phys. Soc. Jpn.* 63: 4070 (1994).
- 16) K. Nagayama, *J. Phys. Chem. Solids*, 58: 271 (1997).
- 17) K. Nagayama, Y. Mori, *J. Appl. Phys.* 84: 6592 (1998).
- 18) J. C. Slater, *Introduction to Chemical Physics* (McGraw-Hill, New York, 1939), Chap. XIII.
- 19) J. S. Dugdale and D. K. MacDonald, *Phys. Rev.* 89: 832 (1953).
- 20) V. Ya. Vaschenko, and V. N. Zubarev, *Sov. Phys. Solid State*, 5: 653 (1963).
- 21) J. J. Dick, R. N. Mulford, W. J. Spencer, D. R. Pettit, E. Garcia, and D. C. Shaw, *J. Appl. Phys.* 70: 3572 (1991).
- 22) Z. A. Dreger, Y. A. Gruzdikov, Y. M. Gupta, *J. Phys. Chem. B*, 106: 247 (2002).
- 23) J. L. Maienschein, P. A. Urtiew, F. Garcia, J. B. Chandler, *AIP Conference Proceedings* (1998), 429 (Shock Compression of Condensed Matter-1997), 711-714.